

Momentum Distributions Of Projectile Residues: A New Tool To Investigate Fundamental Properties Of Nuclear Matter

M. V. Ricciardi^{a,*}, L. Audouin, J. Benlliure^b, M. Bernas^c, E. Casarejos^b, T. Enqvist^{a,1}, B. Fernández, V. Henzl^{a,2}, A. Kelić^a, P. Napolitani, J. Pereira^b, K.- H. Schmidt^a, J. Taïeb^{c,3}

^a*GSI, Planckstr. 1, 64291, Darmstadt, Germany*

^b*University of Santiago de Compostela, 15706 Santiago de Compostela, Spain*

^c*Institut de Physique Nucléaire, 91406 Orsay Cedex, France*

As background experiments for the measurement of the spallation and fission products of uranium and lead, the reactions ^{238}U on lead, ^{238}U on titanium, ^{208}Pb on titanium at 1 A GeV, and ^{208}Pb on titanium at 0,5 A GeV were investigated in inverse kinematics at the Fragment Separator (FRS) at GSI. The use of the FRS, a high-resolution forward magnetic spectrometer, provided new and interesting results concerning the equation of state (EOS) of the nuclear matter, a field generally investigated with 4π devices. In this contribution we will present one of the most important results: the experimental evidence of a re-acceleration of projectile spectators. With increasing mass loss, the longitudinal velocities of the spectators first decrease, as expected from previously established systematics, then level off, and finally increase again. Light fragments are even faster on the average than the projectiles. This finding was interpreted as the response of the spectators to the participant blast. This extremely interesting result was achieved thanks to a distinctive feature of the FRS: the capability to provide extremely precise measurements of the momentum distributions of projectile fragments.

Introduction

The fundamental macroscopic properties of the nuclear matter, like its response to pressure, volume and temperature, are described by mean of the equation of state (EOS). Besides fundamental nuclear-physics aspects, the EOS touches on important questions in astrophysics and cosmology, e.g., the dynamics of supernova explosions¹⁾, the stability of neutron stars under gravitational pressure²⁾ and the nature of matter that existed in the early universe³⁾.

In nuclear physics, important efforts have been spent in the last decades to properly formulate the EOS, in order to describe correctly fundamental properties of nuclear matter like its incompressibility^{4,5)} or its passage through a liquid-gas phase transition^{6, 7)}. The experimental methods for the investigation of the EOS are mostly based on the study of the collisions of heavy ions at relativistic energies. In such experiments some profitable conditions are reached. In the participant zone (“fireball”) high densities and pressures are reached, making this zone adequate for the investigation of the nuclear incompressibility. In the spectators the surviving nuclei acquire excitation energy, and can undergo a liquid-gas phase transition. Intensive effort has been invested to extract information on the EOS by observing light particles emerging from central collisions in full-acceptance experiments (e.g. ref.^{4,5)}) or by studying the statistical behaviour of the spectator matter^{6,7)}. In both cases – the study of nuclear incompressibility and the study of the liquid-gas phase transition – 4π devices or large-acceptance magnetic spectrometers were used, in order to fully recorder the entire production yield. These experimental equipments provide a complete overview on the particle and nuclei produced, but cannot be extremely precise on the measurements of specific quantities, like for instance the momentum distribution of the surviving residues.

* E-mail address: m.v.ricciardi@gsi.de

¹ Present address: University of Jyväskylä, 40351 Jyväskylä, Finland

² On leave from Nuclear Physics Institute ASCR, Řež, 25068, Czech Republic

³ Present address: CEA/Saclay DM2S/SERMA/LENR, 91191 Gif/Yvette CEDEX, France

In this scenario, we propose the use a forward focussed, high-resolution, magnetic spectrometer – the Fragment Separator⁸⁾ – to investigate the influence of the participant zone on the spectator nuclei, and to extract information on the EOS of the nuclear matter.

The experiments

In the frame of the HINDAS project, measurements of formation cross-sections of spallation and fission products of ^{238}U and ^{208}Pb were performed at the FRS at the GSI. The experiments were performed in inverse kinematics, i.e. shooting ^{238}U and ^{208}Pb beams on a hydrogen target (see dedicated talks of this workshop). The study of the reaction ^{238}U on lead at 1 A GeV was performed in advance as a test experiment. The study of the reactions ^{238}U and ^{208}Pb on titanium was necessary to obtain the HINDAS data, since the liquid-hydrogen target was enclosed in a container with titanium windows, and thus the measured nuclide production had to be corrected for the reactions of the beam projectiles in the windows.

The SIS18 heavy-ion accelerator of GSI, Darmstadt, was used to provide a ^{238}U beam of 1 A GeV and two ^{208}Pb beams of 0,5 and 1 A GeV. The beams impinged on two different targets, a 41 mg/cm² titanium target and a 50.5 mg/cm² lead target. In both cases, a 9 mg/cm² aluminium beam monitor acted as an additional target material. In the target layers used in the experiments, the primary beam loses a few percent of its energy; thus corrections due to energy loss in the target do not deteriorate the accurate measurement of the longitudinal momenta of the reaction residues. The reaction products entered into the fragment separator, used as a high-resolution magnetic spectrometer. Full identification in mass and atomic number of the reaction residues was performed by determining the mass-over-charge ratio A/Z from the magnetic rigidity and the time-of-flight, and by deducing the atomic number Z from a ΔE measurement with an ionisation chamber. The acceptance of the fragment separator is about 3 % in momentum and 15 mrad in angle around the beam axis. Measurements with different magnetic fields were combined to fully cover the momentum distributions of all residues. Details of the experimental set-up, in particular the fragment separator and the detector equipment^{9,10)}, as well as a description of the analysis method^{11,12,13)} are given in previous publications.

Once the reaction residue is identified, the measurement of the magnetic rigidity, deduced from the horizontal position at the intermediate dispersive image plane of the fragment separator gives a precise information on its longitudinal momentum p and its velocity v according to the relation:

$$p = m_0 \cdot \gamma \cdot v = B \cdot \rho \cdot Z \cdot e \quad (1)$$

where m_0 is the rest mass of the residue, $-e$ the electric charge of the electron, B is the magnetic field and ρ the bending radius in the dipoles of the first stage of the fragment separator. With the speed of light c , the Lorentz parameter γ is implicitly defined by:

$$\gamma = \sqrt{\frac{1}{1 - v^2/c^2}} \quad (2)$$

The magnetic fields are measured by Hall probes with a relative precision of 10^{-4} . The bending radius ρ is deduced from the position at the intermediate image plane with a statistical relative uncertainty of $\pm 5 \cdot 10^{-4}$, based on a resolution of ± 3 mm in the position measurement. This results in an uncertainty of $\pm 5 \cdot 10^{-4}$ in the momentum of individual reaction products. Systematic uncertainties will be discussed later.

The results

The essential result of the experiments is the systematic scan of the velocity distributions of all the measured reaction residues, from mass ~ 40 to the mass of the projectile.

A nuclide of a given mass and charge can be produced by different reaction mechanisms, namely fragmentation and fission. What is actually observed at the FRS is the longitudinal component of the velocity of residues produced at about zero degrees. In figure 1-b the distribution of the longitudinal velocity of ^{94}Zr produced in the reaction ^{238}U on lead at 1 A GeV is presented in the beam frame. The velocity of ^{94}Zr fragmentation residues fluctuates around the value of the velocity of the pre-fragment, thus its distribution is represented in the beam frame by a full, diffuse sphere. When ^{94}Zr is produced in a fission event, the Coulomb force that acts between the two fission fragments mostly determines its velocity. As a consequence, the possible values of its velocity cover only the external shell of a large sphere. Because of the limited angular acceptance of the FRS (15 mrad around 0°), represented by a cone in the laboratory frame (see figure 1-a), only part of the real production - that one inside the cone - is actually observed.

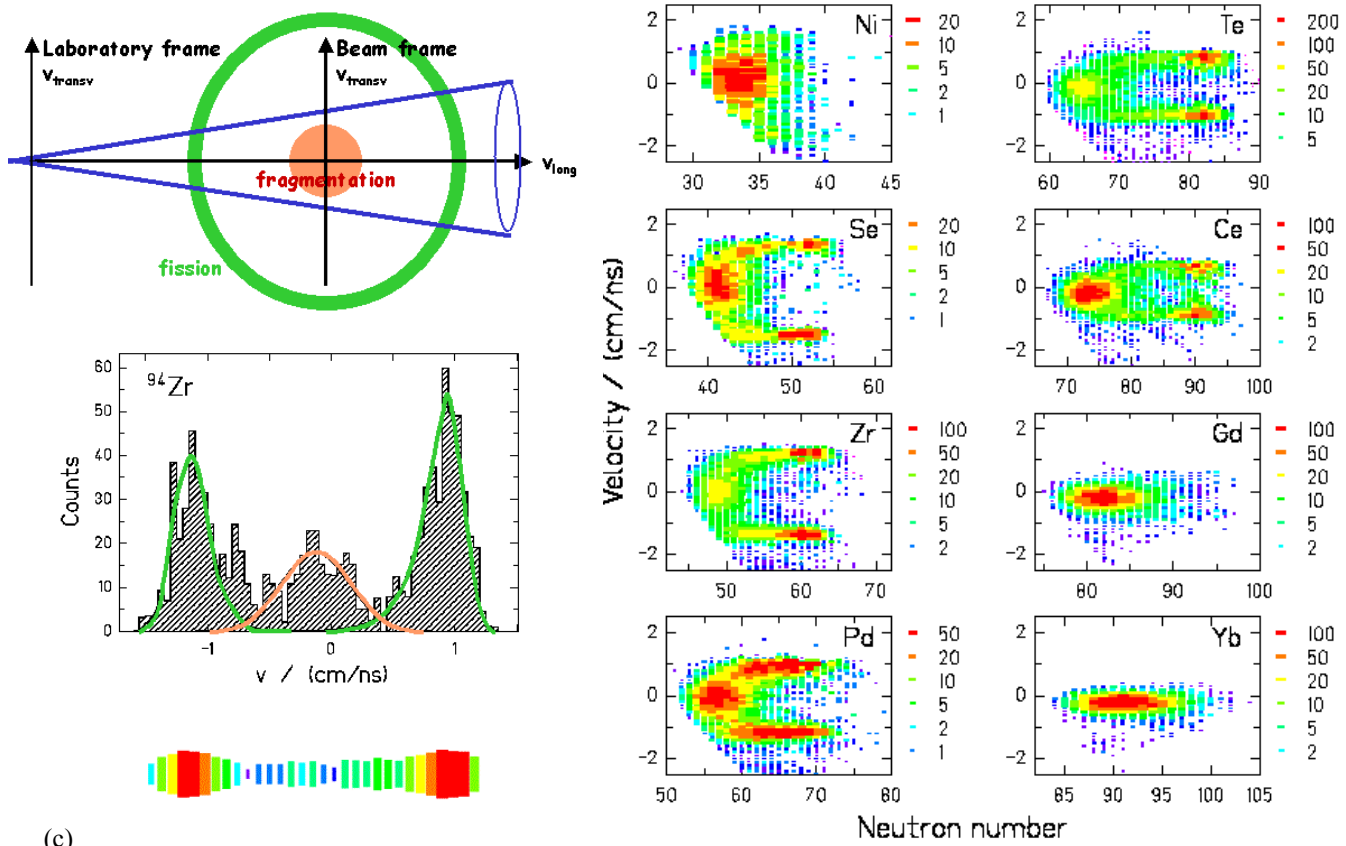


Figure 1: (a): schematic drawing of the transmitted velocities of ^{94}Zr , produced by fission (external shell) or via fragmentation (full sphere). The velocities are presented in the beam frame ($v_{238\text{U}} = 0$ cm/ns). The cone represents the acceptance of the FRS. (b): projections of the velocities on the longitudinal axis. (c): cluster-plot of the velocity distribution. (d): Cluster-plot of the velocity distributions of the isotopes of 8 elements produced in the reaction $^{238}\text{U} + \text{Pb}$ at 1 A GeV.

The angular transmission for projectile fragments ranges from 100 % for $A > 175$ over more than 90 % for $A = 75$ to about 46 % for $A = 40$. The angular transmission for fission fragments is lower. They can only pass the separator when they are emitted close to the forward or backward direction. Projecting the transmitted events on the longitudinal axis, we obtain two narrow velocity distributions at the sides and a broader one in the center (figure 1-b). The triple humped velocity distribution is presented in form of cluster-plot in figure 1-c. Figure 1-d shows the two-dimensional cluster plots of the velocity distributions of the isotopes of eight elements from the reaction $^{238}\text{U} + \text{Pb}$, measured at 1 A GeV. The most neutron-rich isotopes predominantly appear in two narrow velocity ranges, corresponding to fission in forward and backward direction. The most neutron-deficient isotopes, which are produced by fragmentation, however, are found close to the beam velocity. The separation between fragmentation and fission residues, previously achieved by recording the associated charged-particle multiplicity¹⁴⁾, is performed in the present experiments by the pattern in velocity and neutron excess as demonstrated in figure 1.

The production of the same nuclides by fission and fragmentation allows for directly comparing their velocity distributions, leading to a very interesting result. The fission products result from fission of very heavy nuclei close to the projectile, produced in very peripheral collisions or by electromagnetic excitations, as deduced from an analysis of their velocity distributions¹²⁾. Although the fragmentation products are expected to be produced in more violent collisions, they appear with higher average velocities. This is particularly striking for selenium and zirconium.

The most probable velocities of fragmentation products as a function of the fragment mass are shown in figure 2 for the four measured systems. The values presented in figure 2-left were already published¹⁵⁾, while those in figure 2-right are yet preliminary data^{16,17)}. Since the mean nuclear charge of the fissioning system could be determined from the observed velocities of the fission fragments¹²⁾, the mean velocity of the fission fragments was used to check the absolute velocity calibration, assuming the validity of the Morrissey systematics¹⁸⁾ in the range of the fissioning systems. The overall systematic uncertainty results to less than ± 0.1 cm/ns for each system, independently.

Three striking findings are observed in figure 2: Firstly, the generally found reduction of the mean velocities, represented by the Morrissey's systematics (green lines) levels off with increasing mass loss in the reaction, and then the velocities tend to increase again. Secondly, these features appear more strongly for the heavier target. Thirdly, these features appear more strongly at higher incident beam energy.

Interpretation

The consequence of the first result is extremely interesting.

The mean velocities of the lighter fragmentation products tend to level off and finally increase again with increasing mass loss. The lightest fragments are found to be even faster than the projectiles. This finding is in contrast to the expectation that lighter products, which are assumed to be produced in more violent collisions, are slowed down in the reactions, since they experience more friction in the nucleus-nucleus collision. We interpreted these results in the light of the theoretical work of Shi, Danielewicz and Lacey¹⁹⁾. According to ref.¹⁹⁾ the velocity of the spectator is modified not only by the friction experienced in the collision stage, but also by the expansion of the fireball, which pushes on the backside of the spectator nuclei. Parameters like the masses of the colliding nuclei and the beam energy might have a strong influence on the magnitude of the fireball blast. This might explain why the acceleration effects observed in Figure 2 appear to be stronger in the case of heavier targets and higher beam velocity. Also the large spreading in the Morrissey systematics of previous data (see figure 8 of ref.¹⁸⁾) for light fragments could find here a natural explanation.

The experimental findings of figure 2, along with the theoretical work of ref.¹⁹⁾, shed a new light on the systematics of previously measured data: The velocities of residues far from the projectile cannot simply be scaled by the mass loss.

In the light of the findings of ref.¹⁹⁾, another interesting consequence emerge from the data: the acceleration found for relatively small impact parameters, presumably leading to the production of light reaction residues, is sensitive to the momentum-dependence of the nuclear mean field. According to the theoretical work of ref.¹⁹⁾, the momentum change of the spectators (and in particular the change in longitudinal momentum) is extremely sensitive to the momentum dependence of the nuclear mean field, but it is not sensitive to the stiffness of the EOS. This can be seen in figure 9 of ref.¹⁹⁾. Quantitatively the effects observed in the present experiments cannot be directly compared to the available calculations of ref.¹⁹⁾. The calculations refer to the systems $^{124}\text{Sn} + ^{124}\text{Sn}$ from 250 to 1000 A MeV and for $^{197}\text{Au} + ^{197}\text{Au}$ at 1000 A MeV. These calculations predict a sizeable post-acceleration effect. The post-acceleration effect in the calculations is stronger by 10 to 20 A MeV/c in the center-of-mass system, corresponding to about 0.25 to 0.5 cm/ns in velocity in the projectile frame, if momentum-dependent cross sections are used, compared to calculations with momentum-independent cross sections. This is in the order of magnitude of the effects observed in the present experiments. For a more quantitative assessment, dedicated calculations of the systems studied in the present work would be required. According to the model calculations of Shi, Danielewicz and Lacey, the peculiar nature of the longitudinal momentum as an observable is the selective sensitivity to the momentum dependence of the mean field. This property is rather unique compared to most experimental signatures, which are sensitive to both, the hardness of the equation of state and the momentum dependence of the mean field. Also the transversal momentum of the spectator, which was not measured in the present experiments, is sensitive to both properties.

Conclusions

The high-precision measurement of the velocity distributions of the remnants of the projectile in the reactions $^{238}\text{U} + \text{Pb}$ and $^{238}\text{U} + \text{Ti}$ and $^{208}\text{Pb} + \text{Ti}$ at 500 and 1000 A MeV revealed a surprising result: contrary to what expected according to the previously established systematics¹⁸⁾, the velocities of the fragmentation products do not decrease any more if the mass loss becomes large. The velocities of the very light fragments even tend to increase, until finally they are even faster than the projectiles. This effect is more pronounced for the reaction with the heavier target and with higher kinetic energy.

We interpreted these results as the experimental evidence of the re-acceleration of the spectator fragment by the participant blast, postulated by Shi, Danielewicz and Lacey¹⁹⁾. In the framework of this theoretical work, the precise measurement of the kinematical properties of the spectators represents a new tool to determine the in-medium nucleon-nucleon interactions. The present experiments support the feasibility of this method. As stated in ref.¹⁹⁾, this kind of data will give new information on the equation of state of nuclear matter.

Finally, these results open a new technical approach for the investigation of the EOS of nuclear matter: the use of high-resolution spectrometers for the precise analyse of the velocity distributions of projectile fragments from relativistic heavy-ion collisions.

Discussions with P. Danielewicz are gratefully acknowledged. The work has been supported by the European Community programme "Access to Research Infrastructure Action of the Improving Human Potential" under the contract HPRI-1999-CT-00001.

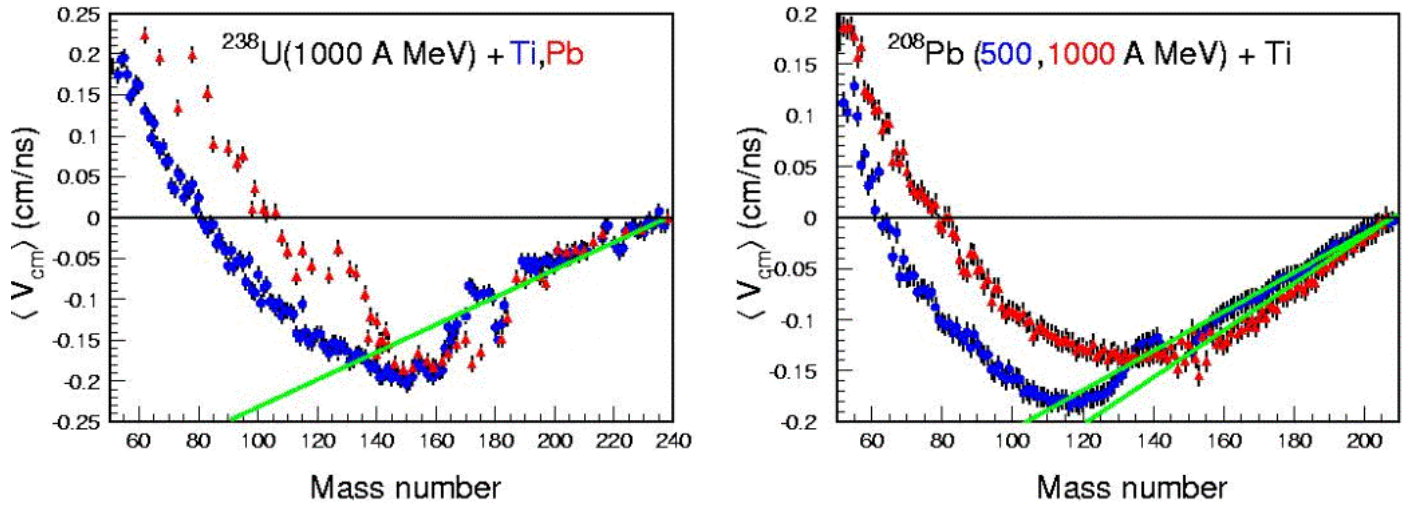


Figure 2: Left: Mean values of the velocity distributions of reaction residues, excluding fission, produced in $^{238}\text{U} + \text{Pb}^{12)}$ (red triangles) and $^{238}\text{U} + \text{Ti}^{15)}$ (blue points) at 1 A GeV in the frame of the projectile. Right: Mean values of the velocity distributions of reaction residues, excluding fission, produced in $^{208}\text{Pb} + \text{Ti}$ at 500 A MeV¹⁶⁾ (blue points) and at 1 A GeV¹⁷⁾ (red triangles) in the frame of the projectile. The green lines represent the Morrissey's systematics¹⁸⁾.

¹ M. Liebedörfe et al., Phys. Rev. **D 63** (2001) 103004.

² M. Prakash et al., Phys. Rep. **280** (1997) 1.

³ D. Boyanovsky, hep-ph/0102120.

⁴ C. Sturm et al., Phys. Rev. Lett. **86** (2001) 39.

⁵ W. Reisdorf, H. G. Ritter, Annu. Rev. Nucl. Part. Sci. **47** (1997) 663.

⁶ J. Pochodzalla and W. Trautmann, in Isospin Physics in Heavy-ion Collisions at Intermediate Energies, Bao-An Li and W. Udo Schröder eds., Nova Science Publishers, ISBN 1-56072-888-4.

⁷ A. Schüttauf et al., Nucl. Phys. **A607** (1996) 457.

⁸ H. Geissel et al., Nucl. Instrum. Methods **B 70** (1992) 286.

⁹ B. Voss et al., Nucl. Instrum. Methods **A 364** (1995) 150.

¹⁰ M. Pfützner et al., Nucl. Instr. Meth. **B 86** (1994) 213.

¹¹ M. de Jong et al., Nucl. Phys. **A 628** (1998) 479.

¹² T. Enqvist et al., Nucl. Phys. **A 658** (1999) 47.

¹³ T. Enqvist et al., Nucl. Phys. **A 686** (2001) 481.

¹⁴ A. I. Warwick et al., Phys. Rev. Lett. **48** (1982) 1719.

¹⁵ M. V. Ricciardi et al., Phys. Rev. Lett. **90** (2003) 212302

¹⁶ L. Audouin, private communication.

¹⁷ B. Fernández, private communication.

¹⁸ D. J. Morrissey, Phys. Rev. **C 39** (1989) 460.

¹⁹ L. Shi, P. Danielewicz, R. Lace, Phys. Rev. **C 64** (2001) 034601